

# Effect of Crosslinking on the Properties of Membrane Formulated from Quaternized Chitosan

N.Z. Kassim Shaari\*, M.A.N. Kamarulzaman, N.S.I. Chik  
School of Chemical Engineering, College of Engineering,  
Universiti Teknologi MARA, 40450 Shah Alam, Selangor, MALAYSIA  
\*norinzamiah@uitm.edu.my

## ABSTRACT

Heavy metals are easily absorbed by living things because of their high-water solubility. Adsorption is a popular separation technique that is used to remove heavy metals from water since it is inexpensive, widely available, and ecologically benign. Chitosan's structure includes hydroxyl and amino groups, which make it a popular adsorbent for heavy metals. In this study, quaternization was used to change chitosan and improve its adsorption capacity. As the quaternizing agent, hexadecyltrimethylammonium bromide (TMAB) was employed. After blending the quaternized chitosan with polyvinyl alcohol and polysulfone, a membrane was created, and tetraethyl orthosilicate (TEOS) was used to crosslink it. Tetraethyl orthosilicate loadings of 1, 2, and 4 weight percent were added to the membrane formulation as a crosslinker. The surface morphology and surface charge of the prepared membranes were then described. Antifouling analysis and water permeation were used to test the performances. According to the results, membrane M4 with 4 weight percent TEOS exhibited the best characteristics, especially in terms of surface charge and surface morphology with strong antifouling capabilities. Furthermore, it has the highest water flux attributed to good surface hydrophilicity. The developed membranes may find application in the heavy metal removal phase of water treatment.

**Keywords:** Quaternized Chitosan; Hexadecyltrimethylammonium Bromide; Membrane; Surface Charge; Antifouling

## **Introduction**

Natural elements having a high molecular mass and a density at least five times that of water are found in heavy metals. The groundwater contains heavy metals like zinc, nickel, copper, chromium, iron, magnesium, manganese, molybdenum, and selenium. The environmental contamination caused by these metals appears to have increased the threats to global public health and the environment in the past. Due to the abrupt growth in their use in a range of industrial, agricultural, residential, and technical applications, the number of people exposed has also significantly expanded [1]. The sources of heavy metals in the environment have been identified as the geological field, the industrial sector, the agricultural sector, the pharmaceutical industry, residential discharge, and natural sources [2]. Surface waters, which range from streams and waterfalls to bodies of water, have the potential to carry heavy metals over great distances and to change chemically as they flow due to localized factors [3]. For instance, minerals will oxidize when water flows over sulfide because of a rise in acidity that changes the solubility of heavy metals and so enhances their mobility in the water. The most widely used methods for removing heavy metal components from water bodies nowadays are membrane separation, ionic exchange, coagulation-flocculation, precipitation, and adsorption [4]. Every approach, though, has certain drawbacks. For example, excessive operating expenses, long operating times, generation of secondary pollutants, incompatibility, and intolerance for extensive usage. To remove the secondary chemicals produced before getting safe-treated water, these methods usually require extra separation and filtration [5]. When the amounts of heavy metals in the treated water satisfy Malaysia's National Water Quality Standards, it is deemed safe because the heavy metals are being removed from the water. To make treated water safe to use, any earlier suggested techniques for removing heavy metals from the water can be taken into consideration because they have high removal efficiency despite the abovementioned drawbacks. Among the previously mentioned techniques, the adsorption process is widely used to remove heavy metals from water because it is an inexpensive, readily available, and ecologically beneficial technology. Adsorbents that meet the requirements of having larger surface areas and smaller particle sizes are considered good adsorbents. This kind of adsorbent is what can raise the water's adsorbate-adsorbent interaction and chemical reactivity [6]. Because it is derived from natural resources and has hydroxyl and amino groups that bind metal ions, chitosan (CS) is a well-liked adsorbent for heavy metals. One of the biopolymers, chitosan (CS), is a non-toxic linear molecule with a high molecular weight and the ability to biodegrade [7]. Unfortunately, because of disadvantages including low heat stability, low water solubility, low acid stability, low mechanical characteristics, and resistance to mass transfer, its applicability is limited [8]-[9]. The extraction process and source are the only factors that affect chitosan's characteristics.

Understanding and managing chitosan is essential since it affects the properties and applications of the biopolymer. Surface area, particle size, molecular weight, and degree of deacetylation are the main characteristics that define the quality and range of applications of chitosan [10]. The number of monomeric units in the biopolymer determines the molecular weight (MW) of chitosan. Chitosan properties like viscosity, solubility, and application are influenced by MW. Researchers have found that raising the molecular weight of chitosan can improve the way that synthetic and biopolymers interact. The molecular weight of chitosan also affects its physicochemical properties [10]. A crucial element that determines the characteristics and uses of chitosan is the degree of deacetylation (DD). Like MW, DD affects the properties and applications of chitosan. For instance, the free amino groups on the chitosan polymeric chain increase with increases in DD. Chitosan with different DD can be made by adjusting the deacetylation process's parameters [10]. Other than that, the surface area and particle size of chitosan are important characteristics. These characteristics, which are connected to the chitosan particle's porosity, pore volume, and pore size distribution, rely on the integrated membrane's casting process and source [10]. Chitosan functions as a barrier during the membrane separation process, allowing some materials to flow through while blocking others. Retentate is the term used to describe the rejected element, while permeate refers to the treated and collected streams. This situation illustrates the size exclusion mechanism in the membrane separation process where the membrane from chitosan functions as a physical barrier. Verifying the pore size of the generated membrane can help determine the kinds of pollutants that the membrane is capable of effectively removing where the pollutants larger than the pore size of the membrane will be retained [5]. Quaternized Chitosan (QCS) is prepared to improve the polymer's adsorption capacity, especially for the separation of heavy metals, and to increase its solubility in water [9]. With its special properties including biodegradation, biological activity, low toxicity, and biocompatibility, quaternized chitosan has several uses in environmental domains like wastewater treatment. Chitosan-N-2-hydroxypropyl trimethyl ammonium chloride (HTCC), one of the quaternized chitosans depicted in Figure 1, is a highly effective flocculent and absorbent agent [11].

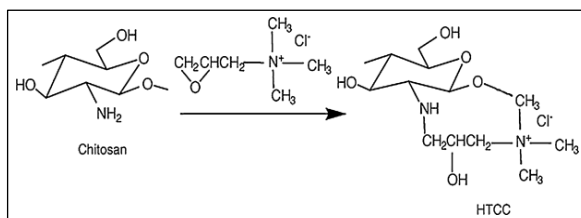


Figure 1: The reaction of producing quaternized chitosan [11]

The solubility of quaternized chitosan is enhanced along with its anti-microbial, anti-coagulant, and antioxidant activities when it has a long-lasting positive charge [12]. The advantage of quaternization of chitosan lies in its ability to progress on the lateral groups while maintaining its primary backbone. This allows chitosan to retain its inherent biological, physical-chemical, and physical characteristics while acquiring new attributes. Quaternized chitosan has the potential to contain more positive charge, which could result in electrostatic repulsion between the chitosan chains, according to Andreica et al. [12]. Apart from that, lateral alkyl chains could be implanted using quaternized chitosan. These two variables, according to the author, had an impact on how the intra- and intermolecular bond connections in the chitosan chains interfered. Quaternized chitosan will therefore have better water solubility and less material stiffness. Due to their ability to achieve superior metal linkage with biodegradable and ecologically acceptable chemicals, the research on utilizing a combination of biopolymers and synthetic polymers for heavy metal ion removal is gaining popularity. For instance, to improve chitosan's integral stability, polyvinyl alcohol (PVA) and polysulfone were combined with it. The polymer blending between QCS/PVA as a hydrophilic polymer with polysulfone as the hydrophobic polymer was conducted to obtain new types of material with a diverse intermediate property between those of pure components, that come together with an economical advantage. Besides its low price and high availability, polysulfone is widely used due to its good physico-chemical, mechanical, and hydraulic stability [13]. As for the quaternization process, the use of hexadecyltrimethylammonium bromide (TMAB) as a quaternizing agent for chitosan in the treatment of wastewater containing both metal anions and cations is essentially undocumented [7]. By its quaternary ammonium surfactant content, TMAB, also known as cetrimonium bromide (CTAB), can easily remove positively charged ions from adsorbents by reducing their surface tension.

In this investigation, tetraethyl orthosilicate was used to crosslink the quaternized chitosan after it was mixed with polyvinyl alcohol/polysulfone. Using tetraethyl orthosilicate (TEOS) as a crosslinker, the study assesses the impact of varying crosslinking degrees on the properties of integral membranes, including surface morphology, surface charge, water flux, and antifouling performance.

## **Experimental Section**

### **Materials**

Sigma Aldrich (M) supplied polyvinyl alcohol (PVA) pellets with a hydrolysis degree ranging from 87% to 89% (MW: 85000 - 124000) and polysulfone resin pellets (MW: 44000 - 53000). Chitosan with a deacetylation degree of  $84.4 \pm$

12% was purchased from Aman Semesta Enterprise located in Shah Alam, Malaysia. The supplier of Dimethyl Sulfoxide (DMSO) was R&M Chemicals, located in Subang, Malaysia. N-Methyl-2-pyrrolidone (NMP) and polyethylene glycol (PEG400) were purchased from Merck Sdn. Bhd. in Selangor, Malaysia. BT Science Sdn. Bhd. supplied the following products: 99% pure tetraethyl orthosilicate (TEOS), hexadecyltrimethylammonium bromide (TMAB), potassium hydroxide solution (KOH), 37% pure hydrochloric acid (HCl), and 2wt% acetic acid. All the chemicals were used without further purification.

## **Methods**

### **Preparation of Quaternized Chitosan (QCS)**

99.5 g of 2 wt.% acetic acid and 0.5 g of chitosan were dissolved at 90 °C while being continuously stirred at 400 rpm for four hours. Following that, 10 g of TMAB were added to the solution when it had cooled to 65 °C. Next, 15g of KOH solution was added all at once to the mixture, which was continuously agitated at 400 rpm. The mixture was then heated for four hours at 400 rpm and 65 °C while being continuously stirred. White quaternized chitosan precipitates were obtained by filtering the resulting solution through filter paper and rinsing it with 100 mL of ethanol.

### **Preparation of hybrid membrane solution**

PVA solution and QCS were combined at a weight ratio of 1:10 [14]. This was achieved by mixing 50 g of the PVA solution with 5 g of the QCS white precipitate. As a crosslinker, 1 weight percent of TEOS was then added to the mixture. Then, 1 millilitre of 37-weight percent HCl was added to catalyze the sol-gel reaction. After that, the mixture was heated to 60 °C and stirred for six hours at 400 rpm. The procedure was repeated with and without the addition of TEOS, utilizing 2 and 4 weight percent TEOS.

### **Preparation of polysulfone solution**

To make a 13 wt.% PSF solution, 13 g of PSF resin pellet, 82 g of NMP solution, and 5 g of PEG 400 were combined [15]. For six hours, the mixture was continuously stirred at 400 rpm and heated to 80 °C. The solution was combined with the hybrid membrane solution after being allowed to cool to room temperature.

### **Preparation of integral membrane**

One gram of the hybrid solution, as shown in Table 1, was combined with forty grams of the polysulfone solution to create the integral membrane. For three hours, the mixture was continuously stirred at 750 rpm while heated to 80 °C [16]. Lastly, the liquid was left to cool before the membrane film was cast. After the solution was applied to a glass plate, a 100 µm-thick film of the

membrane was created using a film applicator. The plate and film were then submerged in a lot of water for a full day.

Table 1: Various formulations of the hybrid membrane solution

Membranes	QCS (g)	PVA (g)	TEOS (g)
M1	5	50	0
M2	5	50	0.55
M3	5	50	1.1
M4	5	50	2.2

Following two days of drying in a room, the membranes were examined using a FESEM to determine their surface morphology and Zeta Potential to measure their surface charge. Their performances were also evaluated using pure water flux and antifouling analyses.

### Characterization of membranes

At magnifications ranging from 10x to 300,000x and with a nearly infinite depth of field, field emission scanning electron microscopy (FESEM), brand Jeol, model JSM-7600F was used for examining the surface morphology of membranes. A Zeta Potential Meter with particle sizer, brand Malvern was used to determine the surface charge of the membrane. The strength of electrostatic interactions between charged surfaces is expressed in terms of zeta potential. It develops at the boundary between the surrounding liquid and a solid. When ions adsorb onto surfaces from the solution or functional groups dissolve on the surface, an aqueous solution is present, and this results in surface charge, which is represented by the zeta potential [17]. Each membrane was immersed in 20 millilitres of ultrapure water for a whole day to ensure the complete generation of electrical potential at the membrane surface when in contact with water before analysis [18]. After the membrane was taken out of the water, the surface charge of the water was measured. The analysis was done by pumping out the water and it was filled into an electrode test cell and placed within a zeta potential meter. Since water was utilized as the dispersant, the refractive index (RI) was 1.333. The zeta potential value was recorded for each membrane. A pH meter was also used to determine the pH of the water samples.

### Performance testing

To test the membranes' pure water flux, membrane filtration equipment with a dead-end filtration mode was employed. Before the membrane sample was put into the stirred cell's porous disc, it was first cut into a circular form with a 19 cm<sup>2</sup> surface area. The feed solution for the stainless-steel stirred cell was 300 mL of deionized water, added before the start of the filtering process. After that, the cell was pressurized to eight bars using nitrogen gas. Samples from

the permeate stream were collected every 15 minutes for an hour, and Equation (1) was then used to calculate the water flux value ( $J$ ).

$$J = \frac{V}{A \cdot \Delta t} \quad (1)$$

where  $V$  is the volume collected ( $L$ ),  $A$  is the cross-sectional area of a membrane ( $m^2$ ) and  $\Delta t$  is the time taken ( $h$ ) for the corresponding volume.

For the antifouling analysis, the same apparatus was utilized, but with a pressure of 10 bars due to this filtration involving a viscous solution of humic acid [19]. There were three stages to the analysis. Deionized water was utilized as the feed solution for the first half hour, and the stabilized flux was designated as  $J_{w1}$ . The following step was filtering with a 200 ppm humic acid solution for an hour. The permeate stream was extracted and the volume was monitored every fifteen minutes. The final flux was recorded as  $J_{HA}$  after an hour. The membrane was submerged in a beaker of deionized water and stirred at 150 rpm for 30 minutes to clean it. We call this procedure as "backwashing." Using the backwashed membrane, the first step was repeated after substituting deionized water for the feed solution.  $J_{w2}$  was the final flux recorded. Equations (2), (3), and (4) were utilized to calculate the fouling resistance characteristics that represented the flow recovery ratio (FRR), irreversible fouling ratio (IFR), and reversible fouling ratio (RFR) [20].

$$FRR = \left( \frac{J_{w2}}{J_{w1}} \right) \times 100 \quad (2)$$

$$RFR = \left( \frac{J_{w2} - J_{HA}}{J_{w1}} \right) \times 100 \quad (3)$$

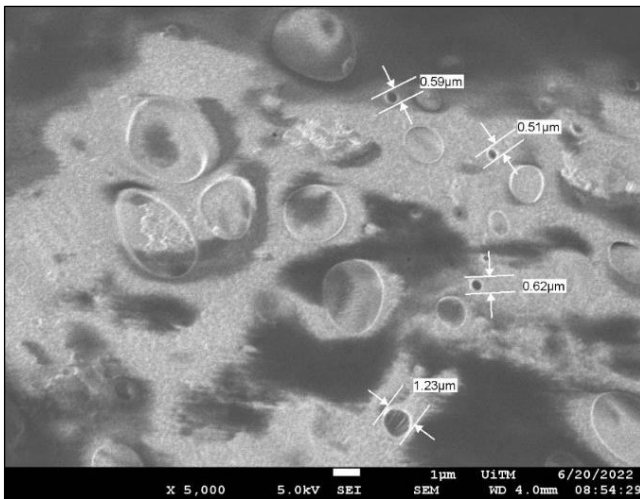
$$IFR = \left( \frac{J_{w1} - J_{w2}}{J_{w1}} \right) \times 100 \quad (4)$$

## Results and Discussion

### SEM analysis

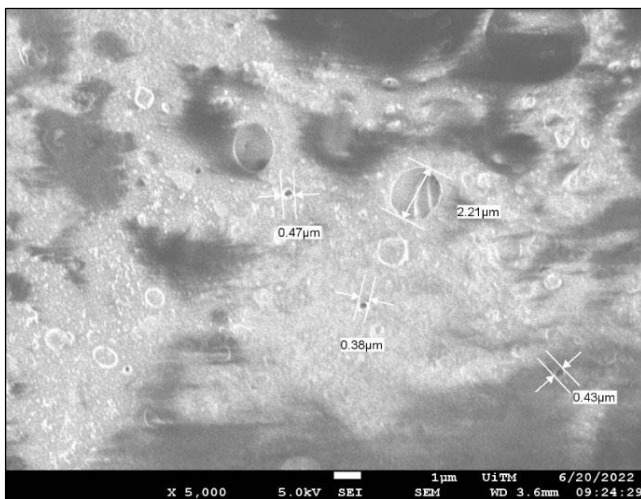
All membranes' surface morphology is shown in Figures 2a–2d. The FESEM pictures demonstrate that the QCS-TMAB was uniformly distributed across the membrane matrix to create a smooth surface [21]. This is due to the addition of TMAB as a cationic substituent might, under physiological conditions, improve the solubility and positive charge density of chitosan by facilitating more efficient binding towards the metal ions if the membrane is to be used in the heavy metal removal process [22]. This situation is due to the separation behaviour of nanofiltration based on both size exclusion and Donnan exclusion theory which describes the exclusion of charged solutes

from penetrating through the membrane [23]. By size exclusion, smaller solutes can pass through the membrane to achieve separation while neutral molecules larger than the membrane hole are more likely to be rejected selectively [24]. The electrostatic interaction between a charged solute and a charged membrane is explained by the Donnan effect. Higher ion concentrations than those in the main solution result from the ions in the solution with the membrane's opposite charge being drawn to the membrane by electrostatic attraction. Certain ions will passively flow across the membrane to preserve electrical neutrality, while ions that have opposite charges to the membrane will be intercepted. As a result, the rejection rate of a charged solute depends on other ions that are present in addition to its electricity and charge [24]. Because of the membrane's rapid crosslinking process, increasing the TEOS concentration reduced the mean pore size. This condition is evident in Figures 2c and 2d, where the pictures do not show any distinct pores. Furthermore, because the hydrophilicity of the membranes was enhanced, it was anticipated that the combination of silica from TEOS and TMAB would strengthen the antifouling capabilities [20]. The result shows that membrane surface M4, which has the least amount of pore creation in the membrane, has the smoothest surface. There was an uneven coloration of the SEM images which might be due to the charging from the membrane because of insufficient coating.

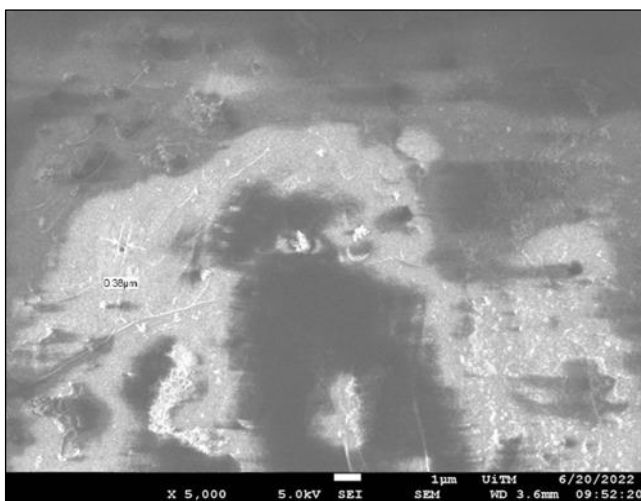


(a)

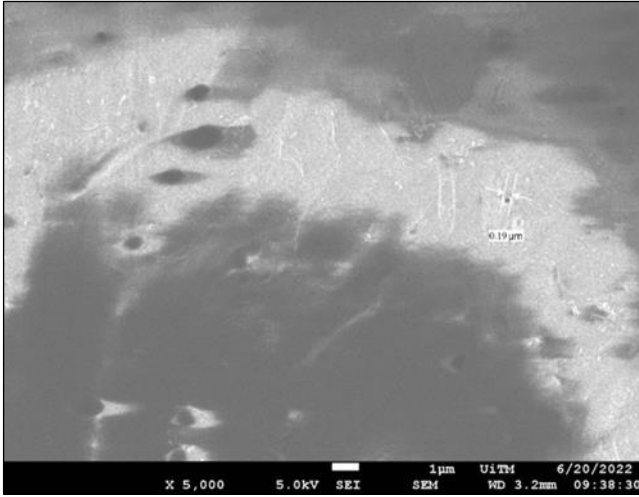




(b)



(c)



(d)

Figure 2: FESEM analysis for; (a) membrane M1, (b) membrane M2, (c) membrane M3, and (d) membrane M4, at 5K magnification

### Pure water flux

Pure water flow can be impacted by the hydrophilicity and structure of membranes [20]. Every membrane's water flux is displayed in Figure 3. According to the results, the water flux has increased due to the presence of TEOS, and the value increases in proportion to the TEOS concentration. The largest flow is found in Membrane M4, which is associated with the membrane's increased surface hydrophilicity and the formation of a macrovoid structure [20]. This circumstance may be connected to the addition of TEOS silica nanoparticles, which have a hydrophilic character with high surface area and porosity to increase the free volume in the membrane polymer matrix to enhance the permeation of water through the membrane [25]-[26] These properties are preferable in the removal process of heavy metal ions as the flux is not jeopardized although the adsorption layer of metal ions increases on the membrane surface.

### Antifouling analysis

Humic acid (HA) solution was used as the foulant model to assess the antifouling properties of the membranes. The related antifouling characteristic values for each membrane are shown in Table 2 in terms of FRR, RFR, and IFR. The table shows that throughout the filtering of HA solution, all membranes exhibit the same trend of flux dropping. The pure membrane shows the maximal flux during the two-hour filtration period, regardless of the kind of solution. M4 exhibits superior antifouling properties compared to the

pure blended membrane, with a higher flux recovery ratio (FRR) of 80.36% and a bigger reversible fouling ratio (RFR) of 42.12%. The antifouling performance in the membrane purification process improves with increasing FRR and RFR values [20]. Moreover, the reduced IFR value demonstrated better pore walls and antifouling properties or less oil absorption on the membrane surface [27]. On the other hand, reversible fouling is acceptable because it may be eliminated with hydraulic cleaning and backwashing to restore water permeance. The membrane with M2 has the lowest RFR (12.74%), suggesting that physical washing was not successful in removing the foulant. With 63.01%, it likewise has the lowest FRR of any membrane. Membrane M1, which has good antifouling characteristics, ranks second after membrane M4. As the membrane's surface became more hydrophilic and the size of its surface pores decreased, the fouling of the membrane decreased. Hence, the membrane's hydrophilic character was the only factor that may affect the antifouling behaviour [28]. Because silica has a hydrophilic character and the membrane's surface has improved hydrophilicity, the concentration polarization phenomenon has been eliminated, particularly for membranes using TEOS.

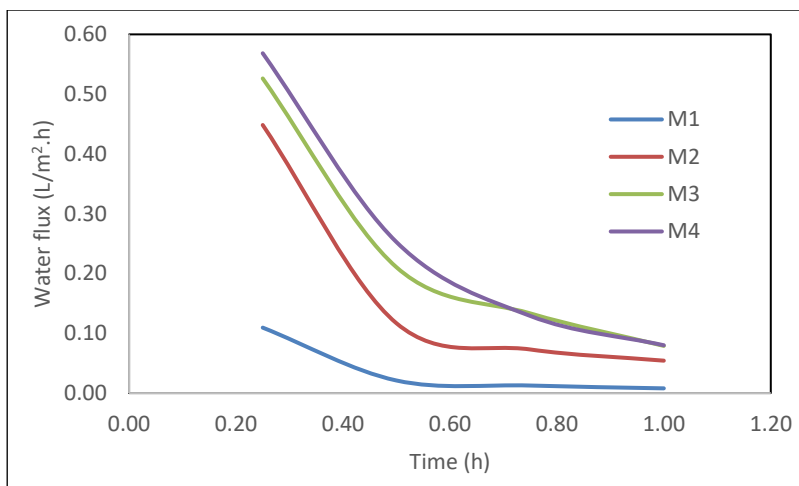


Figure 3: Pure water flux of all membranes

Table 2: The antifouling characteristics of all membranes

	M1	M2	M3	M4
$J_{w1}$ (L/m <sup>2</sup> .h)	80	73	63	56
$J_{w2}$ (L/m <sup>2</sup> .h)	7.6	6.6	5.3	3.5
$J_{w3}$ (L/m <sup>2</sup> .h)	60.5	46	43	45
RFR (%)	25.25	12.74	20.79	42.14
FRR (%)	75.63	63.01	68.25	80.36
IFR (%)	24.38	36.99	31.75	19.64

### Surface charge

The electrochemical equilibrium at the particle-liquid interface is measured by the zeta potential. It is now recognized as one of the key factors influencing the stability of colloidal particles since it measures the strength of electrostatic attraction or repulsion between particles. It should be noted that the term "stability" when used in reference to colloidal dispersions usually means the dispersion's resistance to change over time. The results of zeta potential are shown in terms of surface charge in Table 3. With a charge of -33.95 mV, deionized water was used as the blank sample.

Table 3: Results from zeta potential analysis

Solutions	Zeta potential (mV)
Ultrapure water (UW)	-33.95
UW with M1	-3.06
UW with M2	-24.8
UW with M3	-11.15
UW with M4	-19.80

According to the data, all the formulated membranes are positively charged because the blank sample has the largest negative charge value. The membrane's greatest positive charge is shown by the zeta potential value of -3.06 mV, which is the lowest negative value for membranes without the TEOS (M1). The positive charge of the membrane containing quaternized chitosan is reflected in the zeta potential value of M1 [29]. The negative values of zeta potential increased in comparison to M1, indicating a reduction in positive charge due to the integration of TEOS as a silica nano precursor in the membrane. The quaternized chitosan's electrostatic repulsion towards silica with a negative zeta potential value may be the cause of this circumstance [30]-[31]. However, in comparison to the zeta potential for ultrapure water, the membranes containing TEOS had a positive charge, hence the reduced zeta potential was only slightly higher. The pH-dependent adsorption of hydroxide and hydronium ions from the solution provides a picture of the surface charge; negatively charged hydroxide ions are more favoured to be adsorbed than

positively charged hydroxide ions, leading to largely negative values of the zeta potential [32].

## **Conclusion**

Based on the obtained results, a successful quaternization process of chitosan has been conducted. The use of TMAB as a quaternizing agent has introduced a positive charge to the formulated membrane. The crosslinking of the membrane using TEOS has further enhanced the antifouling properties and hydrophilicity of the membrane. Membrane M4 with 4 wt.% TEOS was the best formulation that exhibited the best performance in terms of pure water flux and antifouling, with the average value of the positive charge. With the outlined properties as stated above, the formulated membranes have the potential to be used for water treatment, particularly in heavy metal removal, which is to be conducted in the future.

## **Contributions of Authors**

The authors confirm the equal contribution in each part of this work. All authors reviewed and approved the final version of this work.

## **Funding**

This work was supported by the “Geran Penyelidikan Khas” [600-RMC/GPK 5/3 (119/2020), Newly Formulated Positively Charged Thin Film Composite Membrane with Rice Husk Ash as the Crosslinker for Lithium Ions Separation from Lithium-Rich Concentrated Solution, 2020].

## **Conflict of Interests**

All authors declare that they have no conflicts of interest.

## **Acknowledgment**

The authors would like to thank the College of Engineering, Universiti Teknologi MARA for providing the facilities to conduct this research and for the publication sponsorship.

## References

- [1] P. B. Tchounwou, C. G. Yedjou, A. K. Patlolla, and D. J. Sutton, "Heavy metal toxicity and the environment", *Experientia Supplementum*, vol. 101, no. 1, pp. 133–164, 2014. [https://doi.org/10.1007/978-3-7643-8340-4\\_6](https://doi.org/10.1007/978-3-7643-8340-4_6)
- [2] Z. L. He, X. E. Yang, and P. J. Stoffella, "Trace elements in agroecosystems and impacts on the environment," *Journal of Trace Elements in Medicine and Biology*, vol. 19, no. 2–3, pp. 125–140, 2005. <https://doi.org/10.1016/j.jtemb.2005.02.010>
- [3] H. Bradl, *Heavy Metals in the Environment: Origin, Interaction and Remediation*. Elsevier, 2005.
- [4] F. Fu and Q. Wang, "Removal of heavy metal ions from wastewaters: A review," *Journal of Environmental Management*, vol. 92, no. 3, pp. 407–418, 2011. <https://doi.org/10.1016/j.jenvman.2010.11.011>
- [5] N. Abdullah, N. Yusof, W. J. Lau, J. Jaafar, and A. F. Ismail, "Recent trends of heavy metal removal from water/wastewater by membrane technologies," *Journal of Industrial and Engineering Chemistry*, vol. 76, pp. 17–38, 2019. <https://doi.org/10.1016/j.jiec.2019.03.029>
- [6] G. Prasannamedha, P. S. Kumar, R. Mehala, T. J. Sharumitha, and D. Surendhar, "Enhanced adsorptive removal of sulfamethoxazole from water using biochar derived from hydrothermal carbonization of sugarcane bagasse," *Journal of Hazardous Materials*, vol. 407, pp. 1–59, 2021. <https://doi.org/10.1016/j.jhazmat.2020.124825>
- [7] X. Song, L. Li, L. Zhou, and P. Chen, "Magnetic thiolated/quaternized-chitosan composites design and application for various heavy metal ions removal, including cation and anion", *Chemical Engineering Research & Design*, vol. 136, pp. 581–592, 2018. <https://doi.org/10.1016/j.cherd.2018.06.025>
- [8] X. Mi, K. S. Vijayaragavan, and C. L. Heldt, "Virus adsorption of water-stable quaternized chitosan nanofibers", *Carbohydrate Research*, vol. 387, pp. 24–29, 2014. <https://doi.org/10.1016/j.carres.2014.01.017>
- [9] Y.L. Qiu, Y. Liu, G. L. Zhang, H. Hao, H. M. Hou, and J. Bi, "Quaternary-ammonium chitosan, a promising packaging material in the food industry", *Carbohydrate Polymers*, vol. 323, p. 121384, 2024. <https://doi.org/10.1016/j.carbpol.2023.121384>
- [10] Guilherme L. Dotto, "General considerations about chitosan", in *Frontiers in Biomaterials Chitosan Based Materials and its Applications*, 1st Ed. Bentham Science, 2017, pp. 3–33. <https://doi.org/10.2174/9781681084855117030004>
- [11] H. Ruihua, Y. Bingchao, D. Zheng, and B. Wang, "Preparation and characterization of a quaternized chitosan," *Journal of Materials Science*, vol. 47, no. 2, pp. 845–851, 2011. <https://doi.org/10.1007/s10853-011-5862-4>

- [12] B.-I. Andreica, X. Cheng, and L. Marin, "Quaternary ammonium salts of chitosan. A critical overview on the synthesis and properties generated by quaternization," *European Polymer Journal*, vol. 139, pp. 1-16, 2020. <https://doi.org/10.1016/j.eurpolymj.2020.110016>
- [13] C. P. Leo, W. P. C. Lee, A. L. Ahmad, and A. W. Mohammad, "Polysulfone membranes blended with ZnO nanoparticles for reducing fouling by oleic acid", *Separation and Purification Technology*, vol. 89, pp. 51–56, 2012. <https://doi.org/10.1016/j.seppur.2012.01.002>
- [14] K.-Y. Chen and S.-Y. Zeng, "Preparation and characterization of quaternized chitosan coated alginate microspheres for blue dextran delivery", *Polymers*, vol. 9, no. 12, pp. 1–12, 2017. <https://doi.org/10.3390/polym9060210>
- [15] N. Z. Kassim Shaari, N. A. Sulaiman, and N. A. Rahman, "Thin film composite membranes: preparation, characterization, and application towards copper ion removal," *Journal of Environmental Chemical Engineering*, vol. 7, no. 1, pp. 1–31, 2019. <https://doi.org/10.1016/j.jece.2018.102845>
- [16] N. S. I. Chik, N. Z. K. Shaari, and S. A. Shamsudin, "The separation of oily water mixture using membrane," *IOP Conference Series: Materials Science and Engineering*, vol. 1176, no. 1, pp. 1–7, 2021. <https://doi.org/10.1088/1757-899x/1176/1/012003>
- [17] Sema Salgın, Uğur Salgın, and N. Soyer, "Streaming potential measurements of polyethersulfone ultrafiltration membranes to determine salt effects on membrane zeta potential," *International Journal of Electrochemical Science*, vol. 8, no. 3, pp. 4073–4084, 2013. [https://doi.org/10.1016/s1452-3981\(23\)14454-3](https://doi.org/10.1016/s1452-3981(23)14454-3)
- [18] B. M. Jun, J. Cho, A. Jang, K. Chon, P. Westerhoff, Y. Yoon, and H. Rho, "Charge characteristics (surface charge vs. zeta potential) of membrane surfaces to assess the salt rejection behavior of nanofiltration membranes", *Separation and Purification Technology*, vol. 247, pp. 117026–117026, 2020. <https://doi.org/10.1016/j.seppur.2020.117026>
- [19] N. Z. Kassim Shaari, N. Abd Rahman, N. A. Sulaiman, and R. Mohd Tajuddin, "Thin film composite membranes: mechanical and antifouling properties," *MATEC Web of Conferences*, vol. 103, pp. 1–10, 2017. <https://doi.org/10.1051/mateconf/201710306005>
- [20] F. Kazemi, Y. Jafarzadeh, S. Masoumi, and M. Rostamizadeh, "Oil-in-water emulsion separation by PVC membranes embedded with GO-ZnO nanoparticles," *Journal of Environmental Chemical Engineering*, vol. 9, no. 1, pp. 104992–104992, 2021. <https://doi.org/10.1016/j.jece.2020.104992>
- [21] K. Divya, D. Rana, S. Alwarappan, M. S. S. Abirami Saraswathi, and A. Nagendran, "Investigating the usefulness of chitosan-based proton exchange membranes tailored with exfoliated molybdenum disulfide

- nanosheets for clean energy applications”, *Carbohydrate Polymers*, vol. 208, pp. 504–512, 2019. <https://doi.org/10.1016/j.carbpol.2018.12.092>
- [22] S. V. Raik, D. N. Poshina, T. A. Lyalina, D. S. Polyakov, V. B. Vasilyev, A. S. Kritchenkov, and Y. A. Skorik, “N-[4-(N,N,N-trimethylammonium)benzyl]chitosan chloride: Synthesis, interaction with DNA and evaluation of transfection efficiency”, *Carbohydrate Polymers*, vol. 181, pp. 693–700, 2018. <https://doi.org/10.1016/j.carbpol.2017.11.093>
- [23] X. Li, C. Zhang, S. Zhang, J. Li, B. He, and Z. Cui, “Preparation and characterization of positively charged polyamide composite nanofiltration hollow fiber membrane for lithium and magnesium separation”, *Desalination*, vol. 369, pp. 26–36, 2015. <https://doi.org/10.1016/j.desal.2015.04.027>
- [24] T. Zhang, W. Zheng, Q. Wang, Z. Wu, and Z. Wang, “Designed strategies of nanofiltration technology for Mg<sup>2+</sup>/Li<sup>+</sup> separation from salt-lake brine: A comprehensive review,” *Desalination*, vol. 546, p. 116205, 2023. <https://doi.org/10.1016/j.desal.2022.116205>
- [25] A. Darmawan, S.N. Putri, H. Muhtar, C. Azmiyawati, “Unveiling the influence of MTMS:TEOS ratios in silica layer membranes enhanced by cetyltrimethylammonium bromide”, *Ceramics International*, vol. 50, no. 7, pp. 11904–11915, 2024. <https://doi.org/10.1016/j.ceramint.2024.01.094>
- [26] C.-C. Ye, Q. An, J.-K. Wu, F. Zhao, P.-Y. Zheng, and N. Wang, “Nanofiltration membranes consisting of quaternized polyelectrolyte complex nanoparticles for heavy metal removal,” *Chemical Engineering Journal*, vol. 359, pp. 994–1005, 2019. <https://doi.org/10.1016/j.cej.2018.11.085>
- [27] Z. Zhu et al., “Antifouling modification of PVDF membranes via incorporating positive-charge tuned quaternized chitosan magnetic particles,” *Journal of Environmental Chemical Engineering*, vol. 11, no. 1, pp. 109192–109192, 2023. <https://doi.org/10.1016/j.jece.2022.109192>
- [28] Y. T. Chung, E. Mahmoudi, A. W. Mohammad, A. Benamor, D. Johnson, and N. Hilal, “Development of polysulfone-nanohybrid membranes using ZnO-GO composite for enhanced antifouling and antibacterial control,” *Desalination*, vol. 402, pp. 123–132, 2017. <https://doi.org/10.1016/j.desal.2016.09.030>
- [29] E. Murugan, C. R. Akshata, R. Ilangovan, and M. Mohan, “Evaluation of quaternization effect on chitosan-HAP composite for bone tissue engineering application”, *Colloids and Surfaces B: Biointerfaces*, vol. 218, p. 112767, 2022. <https://doi.org/10.1016/j.colsurfb.2022.112767>
- [30] Q. Zhang, Y. Hu, Y. Feng, X. Sun, and J. Duan, “Critical role of water in fused silica glass by silica nano powder sintering: Nanoparticle dispersion,” *Journal of Non-Crystalline Solids*, vol. 609, p. 122288, 2023. <https://doi.org/10.1016/j.jnoncrysol.2023.122288>



- [31] A. Kumari, Rakesh Kumar Singh, N. Kumar, R. Kumari, Monalisa, and S. Sharma, “Green synthesis and physical properties of crystalline silica engineering nanomaterial from rice husk (agriculture waste) at different annealing temperatures for its varied applications,” *Journal of the Indian Chemical Society*, vol. 100, no. 5, pp. 100982–100982, 2023. <https://doi.org/10.1016/j.jics.2023.100982>
- [32] J. A. D. Sharabati, S. E. Itler, S. Guclu, D. Y. K. Imer, S. Unal, Y. Z. Menceloglu, I. Ozturk, and I. Koyuncu, “Zwitterionic polysiloxane-polyamide hybrid active layer for high performance and chlorine resistant TFC desalination membranes”, *Separation and Purification Technology*, vol. 282, pp. 119965–119965, 2022. <https://doi.org/10.1016/j.seppur.2021.119965>